VHF RADAR OBSERVATION OF AURORAL *E*-REGION IRREGULARITIES ASSOCIATED WITH MOVING-ARCS

Tadahiko OGAWA

Hiraiso Branch, Radio Research Laboratories, 3601 Isozaki, Nakaminato-shi, Ibaraki 311-12

and

Kiyoshi IGARASHI

Radio Research Laboratories, 2-1, Nukui-Kitamachi 4-chome, Koganei-shi, Tokyo 184

Abstract: Electron density irregularities appearing in the auroral *E*-region during a substorm expansion phase were examined by using a 50 MHz doppler radar at Syowa Station, Antarctica. The following results are obtained. (1) Optical aurora is not always collocated with radio aurora, which suggests that the strong electric field exciting plasma instabilities in the *E*-region does not always have an intimate relation to the magnetospheric electric field. (2) The echoing region is substantially limited within the radar range where aspect angles are between 88° and 92°. (3) The 50 MHz radar wave may undergo a few degrees of refraction due to high electron density. (4) Growth and decay times of the instabilities in accord with changes in electric field strength are a few seconds or less. (5) With increasing electric field, echo intensity and mean doppler velocity increase, and the doppler velocity spectrum changes from a 'diffuse' into a 'discrete' form (two-stream-like spectrum). A possibility of the neutral wind effect modifying electron drifts is suggested. These results are compared with the existing theories and with the radar observations made at other stations.

1. Introduction

VHF-UHF radio waves emitted from the ground can be partially backscattered from the electron density irregularities which appear in the disturbed auroral *E*-region. To study this, we use a tool for diagnosing the lower auroral ionosphere called 'auroral radar' or 'auroral doppler radar' if it has an additional function of doppler-shift detection. A large number of radars have been used, especially in the northern polar region, to study the auroral *E*-region irregularities. Now it is believed that the amplitude and doppler spectrum of radar echoes contain information about irregularity characteristics, irregularity production mechanism(s), auroral electrojet intensity, and even the ionospheric electric field. There is, however, some controversy among investigators about the interpretation of observed results and many problems remain to be solved. Radar observations of the equatorial electrojet have disclosed many interesting features of the plasma turbulence and electrojet dynamics, but these results cannot be directly applied to the auroral electrojet plasma because of the different configuration of the geomagnetic field and because of the more complex behavior

of the auroral electrojet plasma than of the equatorial plasma. Consequently, even now, more radar observations are needed. See a recent review paper of FEJER and KELLEY (1980) and the references therein for detailed descriptions.

In contrast to the many radar facilities in the northern high latitudes, only three VHF doppler radars have been installed in the south polar region in the past; 50 MHz at Siple Station, Antarctica (77°55′S, 83°35′W geographic) (BALSLEY *et al.*, 1977), 53.5 MHz at Slope Point, New Zealand (46°40′S, 169°01′E) (KEYS and JOHNSTON, 1979), and 50 MHz at Syowa Station, Antarctica (69°00′S, 39°35′E) (IGARASHI *et al.*, 1981). By using these radars, some aspects of *E*-region irregularities and auroral dynamics have been studied (OGAWA *et al.*, 1979, 1980, 1982; IGARASHI and TSUZURAHARA, 1981; IGARASHI *et al.*, 1981; UNWIN and JOHNSTON, 1981).

A pulsed doppler radar was installed at Syowa Station in 1978 by adding a function of doppler-shift detection to the previous radar system which could measure only echoing range and echo intensity. This radar has been used for studies of both the spatial correlations between radio and optical auroras (IGARASHI and TSUZURAHARA, 1981) and the simultaneous comparisons of electric fields observed by radar and sounding rockets (IGARASHI *et al.*, 1981).

This paper describes in detail the spatial relations between radio and optical auroras and the characteristics of auroral electrojet plasma turbulence, by using the data of the doppler spectrum, spectral width, echo intensity, and mean doppler velocity of the irregularities appearing during a substorm expansion phase. The important radar system parameters for the present observations are (1) frequency=50 MHz, (2) pulse length=100 μs (range resolution=15 km), (3) pulse repetition frequency =400 Hz (corresponding to a maximum unaliasing doppler velocity of $\pm$600 m/s), (4) approximate half-power beamwidth of the 8-element Yagi antennas for transmitting and receiving=40° in horizontal plane and 45° in vertical plane, and (5) antenna azimuth=180° geomagnetic (toward the geomagnetic south pole). See a paper of IGARASHI *et al.* (1981) for other parameters and for the radar system design.

2. Observations and Discussion

2.1. Morphology of optical and radio auroras

The aurora with which we are concerned here appeared in the premidnight hours on March 27, 1978. This aurora was also a target for the Antarctic sounding rocket (S-310JA-7) experiment. The upper panel in Fig. 1 illustrates the contours of auroral 5577Å (broken curves, 5 k*R* spacing) and 50 MHz radar echo intensities (solid curves, 10 dB spacing) in range-time space. Auroral intensity was measured by a geomagnetic meridian scanning photometer located at Syowa Station. Note that one scan needs 30 s and that for drawing the contour curves the lower border of aurora is assumed to be at about 100 km. Since auroral radar echoes are known to come mostly from altitudes between 100 and 120 km (UNWIN and JOHNSTON, 1981), the spatial relationship between optical aurora and radar echo intensity is discernible in the upper panel in Fig. 1. The extent in range of the radar echoes is narrower than that of the optical aurora and is limited to within a nearly constant range. This limitation of echo range is due to so-called '*aspect sensitivity*' which means that the radar cross-section strongly

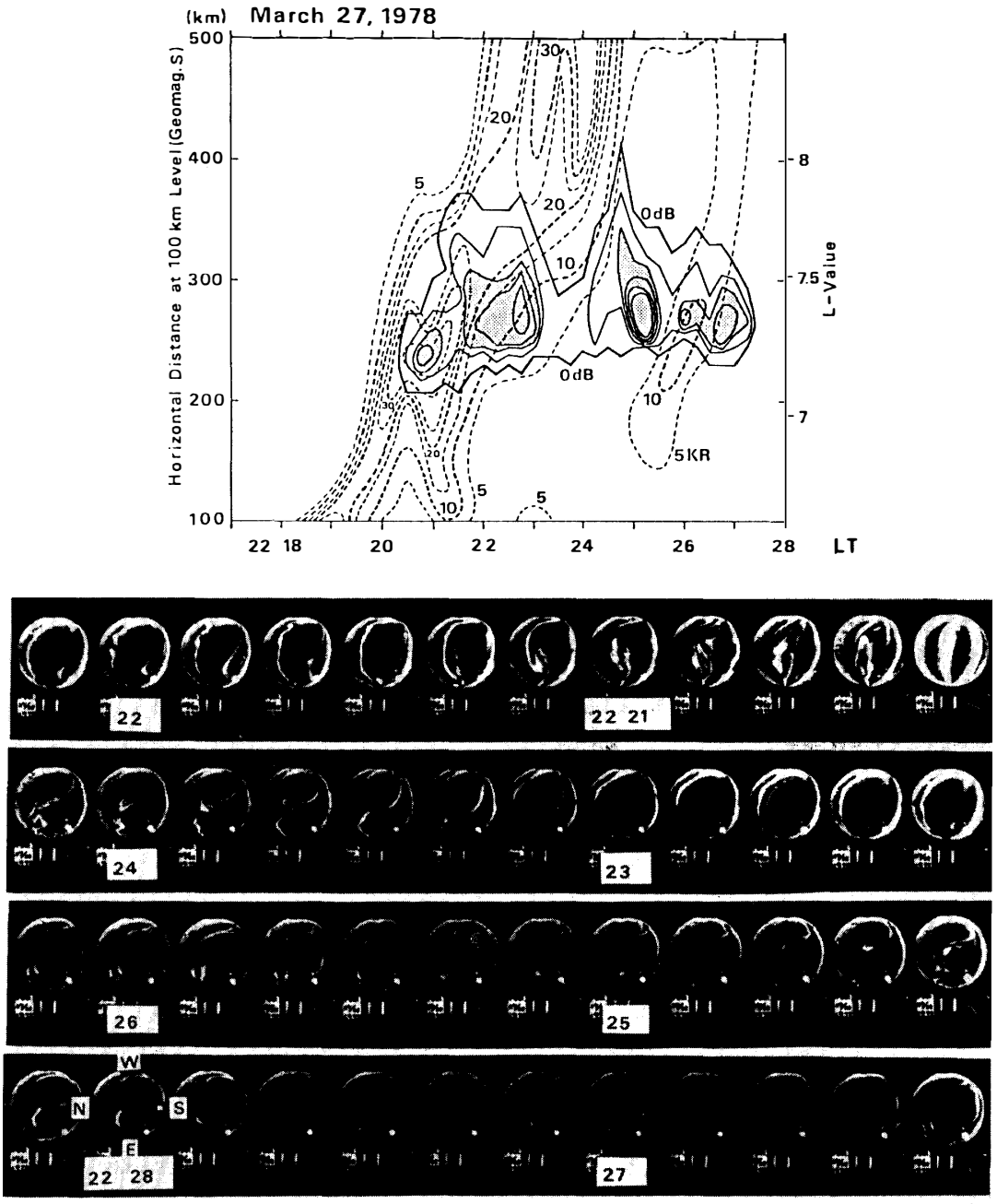

All-Sky Photographs at Syowa Station March 27, 1978

Fig. 1. Contour maps of auroral 5577Å (broken curve, 5 kR spacing) and 50 MHz radar echo intensities (solid curve, 10 dB spacing) in range and time space (upper panel) and all-sky photographs (positive) taken every 10 s (lower panel). These data were taken at Syowa Station. Echo intensity beyond 20 dB is shaded gray in the upper panel. Approximate position of the slant range of 290 km toward geomagnetic south is shown on the 2228 LT all-sky photograph by the white square. The white spot in the south-east quadrant (lower figure) on the all-sky photographs is the moon.

depends on the aspect angle, α, between the radar beam and the geomagnetic field vector. When spatially homogeneous field-aligned irregularities exist, the cross-section becomes maximum for α equal to 90°, abruptly decreasing as α departs from 90°. For the present experiment, α at the 110 km altitude becomes 90° at a slant range of about 290 km which is the distance at which Mizuho Station (70°42′S, 44°20′E) is located. The aspect sensitivity characteristics seen in Fig. 1 will be discussed later in detail in Subsection 3.3. The lower panel in Fig. 1 shows the all-sky photographs taken every 10 s at Syowa Station.

It is seen in Fig. 1 that at 2220: 30 LT (LT=UT+3 h) the radar began to detect the echoes associated with a bright southward-moving arc. The echo intensities were stronger near the center and equatorward side of the arc until 2223 LT. The echoes became faint around 2224 LT with a more southward movement of the arc. An intense echoing region accompanied by no discernible or faint aurora appeared around 2225 LT. This event is interesting indicating that radar echoes are not always correlated with optical aurora. A new arc appeared to the north of the pre-existing echoing region and then moved southward. Echoes associated with this arc were detected at times between 2226 and 2227: 30 LT.

Figure 2 shows the magnetogram and 30 MHz cosmic noise absorption recordings

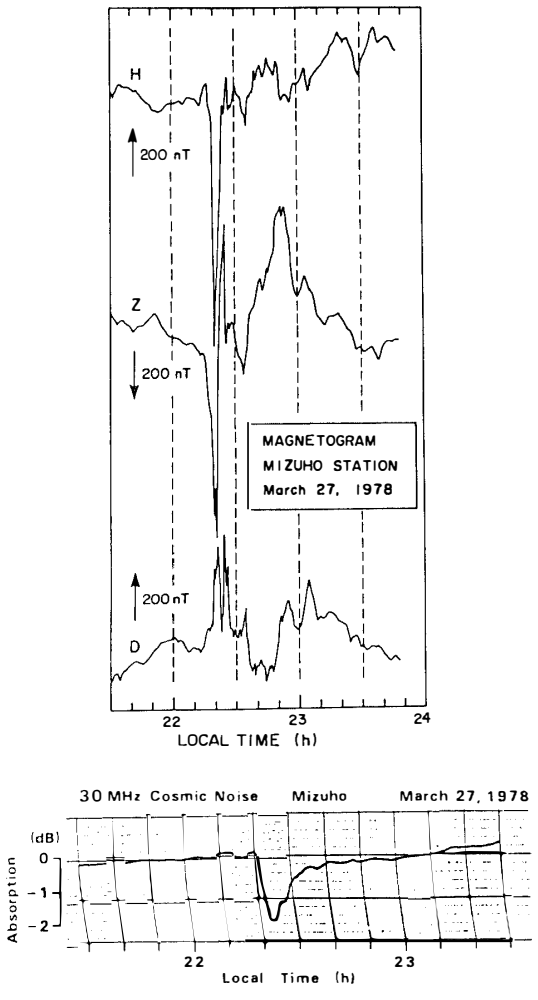

Fig. 2. Three-component magnetogram and 30 MHz cosmic noise absorption recorded at Mizuho Station.

obtained at Mizuho Station. These indicate that the strong westward electrojet current (eastward electron flows) excited by both intense particle precipitation and equatorward electric field were flowing in the bright arc. This result is qualitatively consistent with the *in-situ* measurements of electric fields (OGAWA *et al.*, 1981b) and of energetic electrons (OGAWA *et al.*, 1981a) by a sounding rocket S-310JA-7 which flew within the same bright arc between 2217: 00 and 2217: 30 LT. OGAWA *et al.* (1981b) showed that the DC electric fields in this arc had a strong northward (equatorward) component with a smaller westward component. It is noted that both small-scale electron density irregularities and electric field fluctuations excited by these DC electric fields were measured in the *E*-region by the same rocket (OGAWA *et al.*, 1981a; YAMAGISHI *et al.*, 1981) and that these fluctuations are the primary cause of the VHF radar wave scatterings.

2.2. *Spatial relationships between optical and radio auroras*

Two examples demonstrating spatial relationships between optical and radio auroras are shown in this subsection. The doppler (phase) velocity spectra of 3-m irregularities taken every 15 km in range at the indicated time (every 15 s) are shown in the upper part in Figs. 3a and 3b. A spectrum at every 320 ms was obtained by applying a 128-point fast Fourier transformation technique after analog-to-digital

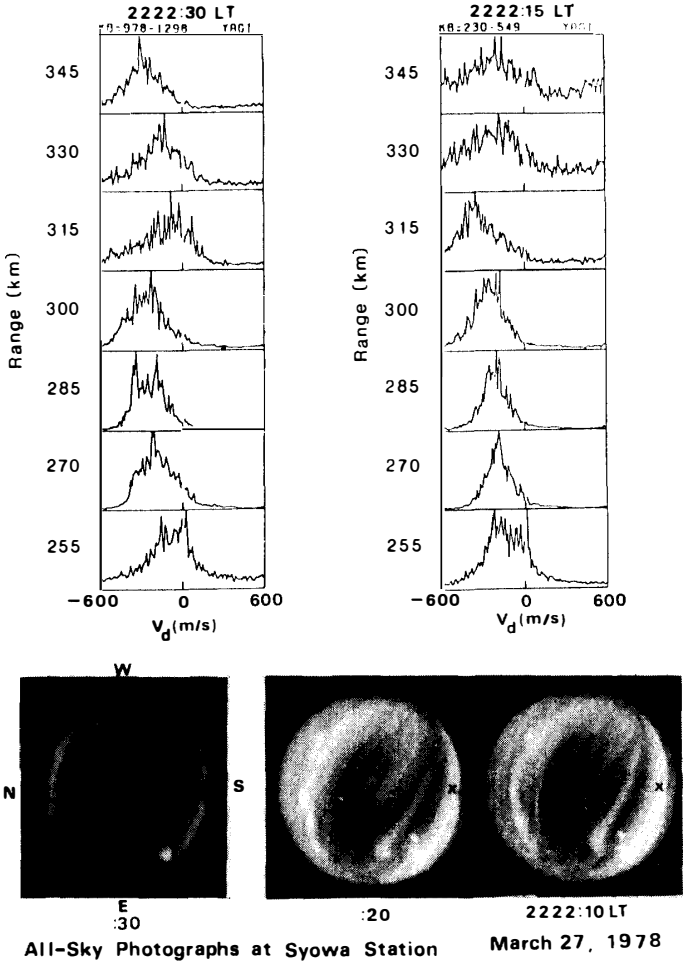

Fig. 3a. Example of good correlations between radio and optical auroras. See text for the doppler spectrum. Approximate position of the slant range of 290 km toward geomagnetic south is shown on the all-sky photographs by the cross.

conversion (sampling rate=10 kHz) of the received analog waveforms of echoes (IGARASHI *et al.*, 1981). Then fourty-five spectra were averaged over 14.4 s to get one averaged-spectrum as shown in Figs. 3a and 3b. A positive sign of doppler velocity means a southward-movement of irregularities away from Syowa Station. The maximum of each spectrum is normalized to unity so that the area below the curve is not proportional to the echo power. See Fig. 6 for the range profiles of echo intensity.

Figure 3a shows an example of good correlations between optical aurora and the echoing region. In fact, the echo intensities were very strong at ranges of 255–315 km at 2222: 15 LT and at ranges of 255–345 km at 2222: 30 LT. The all-sky photographs indicate clearly that these echoes came from the vicinity and inside of the southward-moving bright arc which was elongating in the east-west direction.

An example of poor correlations is shown in Fig. 3b. The echo spectra at 2225: 00 and 2225: 15 LT indicate that there was a strongly irregular region around ranges of 270–315 km where the spectral forms are two-stream-like (see Subsection 3.1). At these times and ranges, however, optical aurora cannot be clearly recognized on the all-sky photographs (see also Fig. 1).

It is known observationally and theoretically that phase velocity vectors of elec-

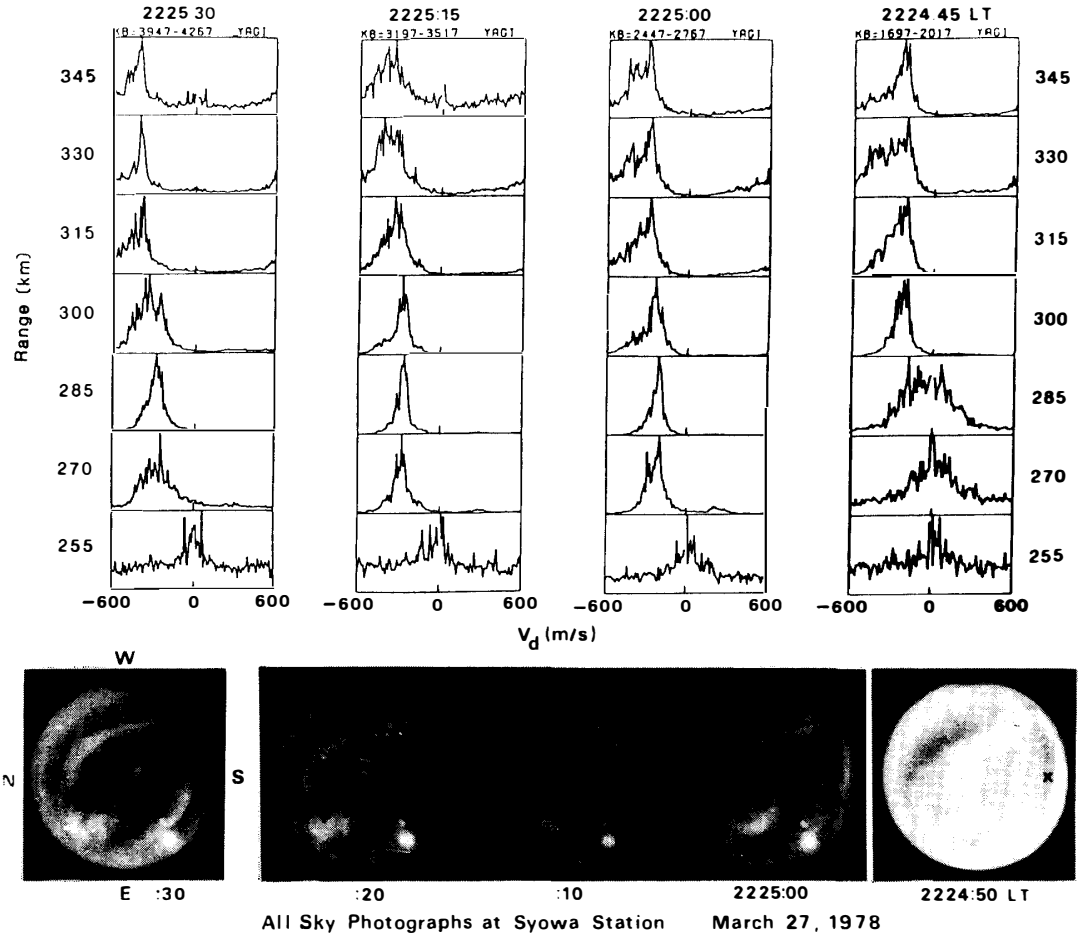

Fig. 3b. Same as Fig. 3a but for poor correlations.

tron density irregularities in the polar *E*-region as seen by VHF radar are approximately given by $\boldsymbol{E}\times\boldsymbol{B}_0/\boldsymbol{B}_0^2$ where $\boldsymbol{E}$ is the electric field vector and $\boldsymbol{B}_0$ is the geomagnetic field vector (ECKLUND *et al.*, 1977; CAHILL *et al.*, 1978). This indicates that in our case the east-west component of $\boldsymbol{E}$, E_{E-W}, can be inferred from the doppler spectrum since the radar beam is directed geomagnetically southward. E_{E-W}(mV/m) is approximately given by $V_d/20$, V_d (m/s) being the doppler velocity. In Figs. 3a and 3b, the doppler velocities are negative, indicating that the electric fields had a westward component. This result is also consistent with the sounding rocket (S-310JA-7) measurement which showed that the east-west component was mostly westward (OGAWA *et al.*, 1981b).

The precipitating electrons with energies of a few keV, which are accelerated somewhere in the magnetosphere by the electric field presumably associated with 'double layers', are the main cause of optical aurora. The ionospheric electric field and/or density gradient are essential driving-forces of the plasma instabilities, such as the two-stream and cross-field instabilities, resulting in the formation of irregularities. Keeping these in mind, a good correlation in location and time between optical and radio auroras may indicate that the magnetospheric electric fields responsible for the auroral particle acceleration are well mapped down into the lower ionosphere along the geomagnetic field lines. On the contrary, it is possible under an imperfect mapping that as a result of spontaneous generation of a closed electric current system in the ionosphere, the irregularities may appear only in a localized region where the ionospheric electric fields are strong (ECKLUND *et al.*, 1977). In this case, a good correlation between optical and radio auroras cannot always be expected. Thus, the correlation study seems to be useful in order to understand the auroral dynamics.

3. Characteristics of Plasma Turbulence

3.1. Diffuse and discrete spectra

The amplitude and doppler spectrum of radar echoes contain much information concerning irregularity characteristics and production mechanisms of irregularities. There are two types of irregularities, type-I and type-II, in the equatorial electrojet. Type-I irregularities are generated by the two-stream instability when the electron drift velocity exceeds the ion-acoustic velocity (300 to 400 m/s in the *E*-region). Type-I irregularity phase velocities measured by VHF radar are near the ion-acoustic velocity due to non-linear processes in a turbulent state, and the spectral width is narrow. Type-II irregularities, on the other hand, are caused by the cross-field instability operating under the combined action of density gradient and electric field. Phase velocities of type-II irregularities are generally slower than the ion-acoustic velocity and the spectral width is wider than that of type-I irregularities. The threshold strength of electric field for the instability is generally lower for the cross-field instability than for the two-stream instability.

The spectra similar to those at the equator were reported in the auroral electrojet (BALSLEY and ECKLUND, 1972; HALDOUPIS and SOFKO, 1976). BALSLEY and ECKLUND (1972) found a third type of spectra which has no similarity to the equatorial type-I and -II irregularities. There is no valid explanation for this type at present.

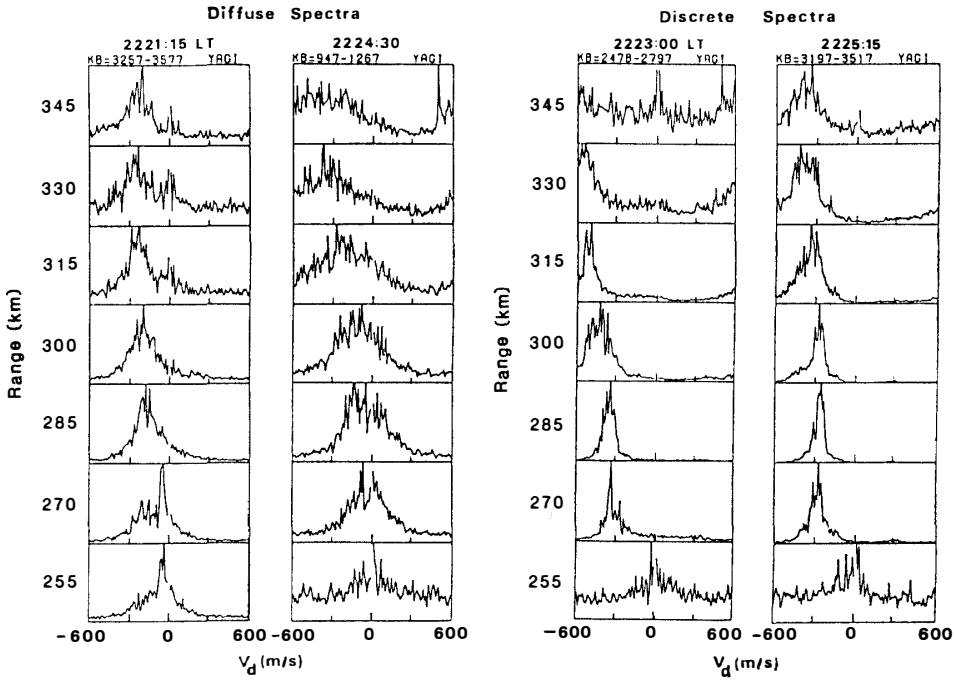

Fig. 4. Examples showing 'diffuse' spectral forms (left) and 'discrete' spectral forms (right). See text for detailed explanation of these spectra.

Figure 4 shows typical examples of two spectral types, diffuse and discrete spectra, found in the present observations. In these examples, the 'diffuse' spectrum (spectra at 285–315 km at 2221: 15 LT and at 270–300 km at 2224: 30 LT) is characterized by a low mean doppler velocity (0 to −200 m/s) (mean doppler velocity implies temporarily here a velocity around which the spectral echo power is maximum), a broad spectral width (greater than 300 m/s), and generally low echo intensity. On the contrary, the 'discrete' spectrum (spectra at ranges of 270, 285 and 315 km at 2223: 00 LT and at 270–300 km at 2225: 15 LT) with generally high echo intensity has a mean doppler velocity of −300 to −500 m/s and a spectral width of about 100 m/s which is narrower than the width in the diffuse spectrum. The discrete and diffuse spectral forms may be compared to the equatorial type-I and type-II irregularity spectra, respectively. However, all spectra obtained here are not always divided into two categories: Some spectra have intermediate characteristics. These results indicate that the electric field and/or the density gradient driving the plasma instabilities were highly variable in space and time for the moving arcs studied here. We note that spectra similar to the third type reported by BALSLEY and ECKLUND (1972) were not found here.

3.2. Growth and decay of irregularities

In order to see how quickly the instabilities causing radar wave scattering grow and decay, the changes in spectral forms with range and time were investigated. Figure 5a shows the spectra, each of which was obtained by averaging fifteen spectra over 4.8 s, during a growth phase of the irregularities. Note that the echo intensities at 240 and 255 km are near the receiver noise level. It is observed in Fig. 5a that the

spectral forms change from the diffuse type into the discrete type within a few seconds, at earlier times for farther ranges. This indicates that the region having strong electric fields capable of exciting the two-stream instability was expanding toward Syowa Station from the south. See Fig. 1 for the associated shift of the strong echoing region toward Syowa Station.

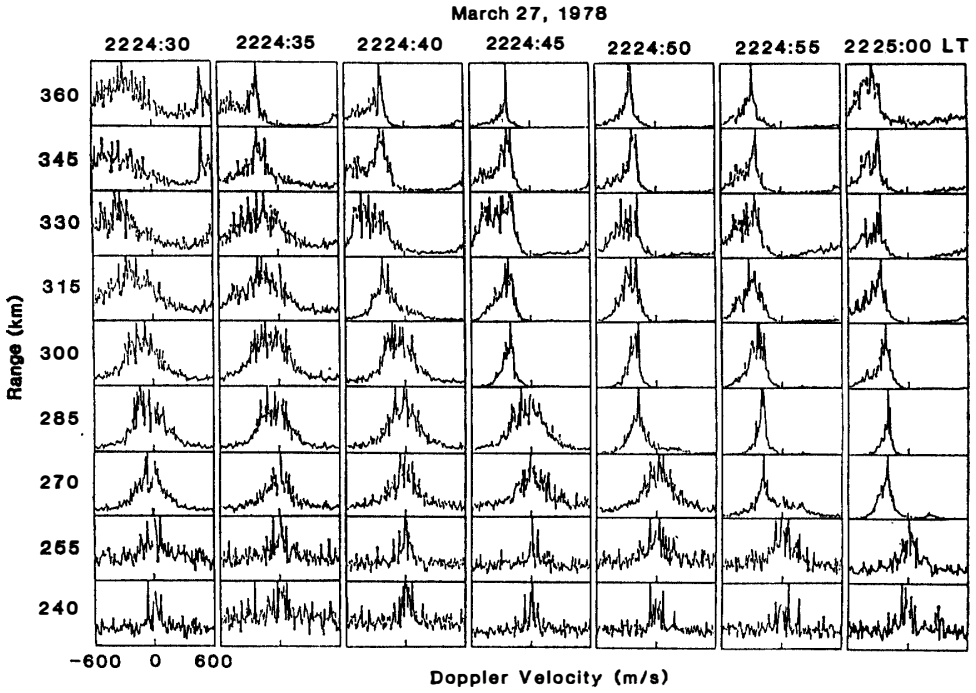

Fig. 5a. Changes in spectral forms with range and time for the growth phase of the irregularities.

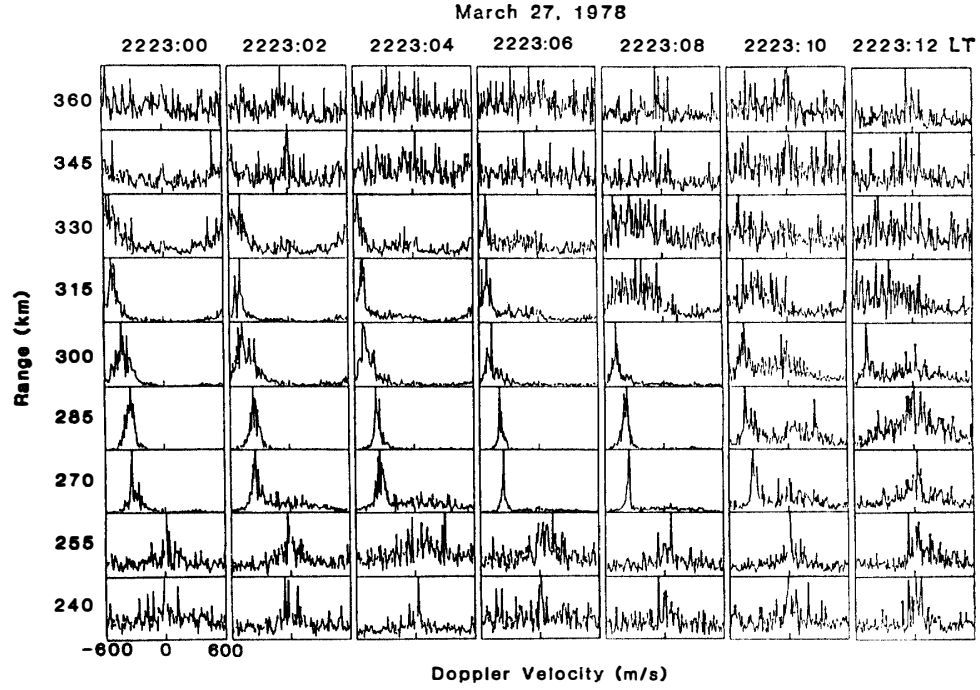

Fig. 5b. Same as Fig. 5a but for the decay phase of the irregularities.

Figure 5b shows the spectra during a decay phase of the irregularities. These spectra were obtained by averaging six spectra over 1.92 s. Note that the echo intensities at 240–255 km and at 330–360 km and after 2223: 10 LT are near the noise level. In this case, the discrete spectra appearing at 270–300 km lose their forms in two seconds around 2223: 09 LT, resulting in noise-like spectra. This suggests that the two-stream instability was shut off due to a sudden decrease in electric field. In fact, it is observed in Fig. 1 that the echo intensities drop sharply around 2223 LT at the equatorward edge of the arc.

3.3. *Range profiles of echo intensity and mean doppler velocity*

The detailed range profiles of echo intensity and mean doppler velocity are presented every 15 s in the left and right panels, respectively, in Fig. 6. These quantities were calculated by applying a double-pulse analysis technique to the received waveforms of echoes (GREENWALD and ECKLUND, 1975). Integration time to get one range-profile is 14.4 s. Mean doppler velocity calculated here represents an 'averaged' velocity of the 3-m irregularities which are regarded as a 'hard' target instead of a 'soft' target and therefore is not necessarily equal to the mean doppler velocity defined in Subsection 3.1. Because of its usefulness, the double-pulse technique has been extensively used for studying auroral dynamics (GREENWALD and

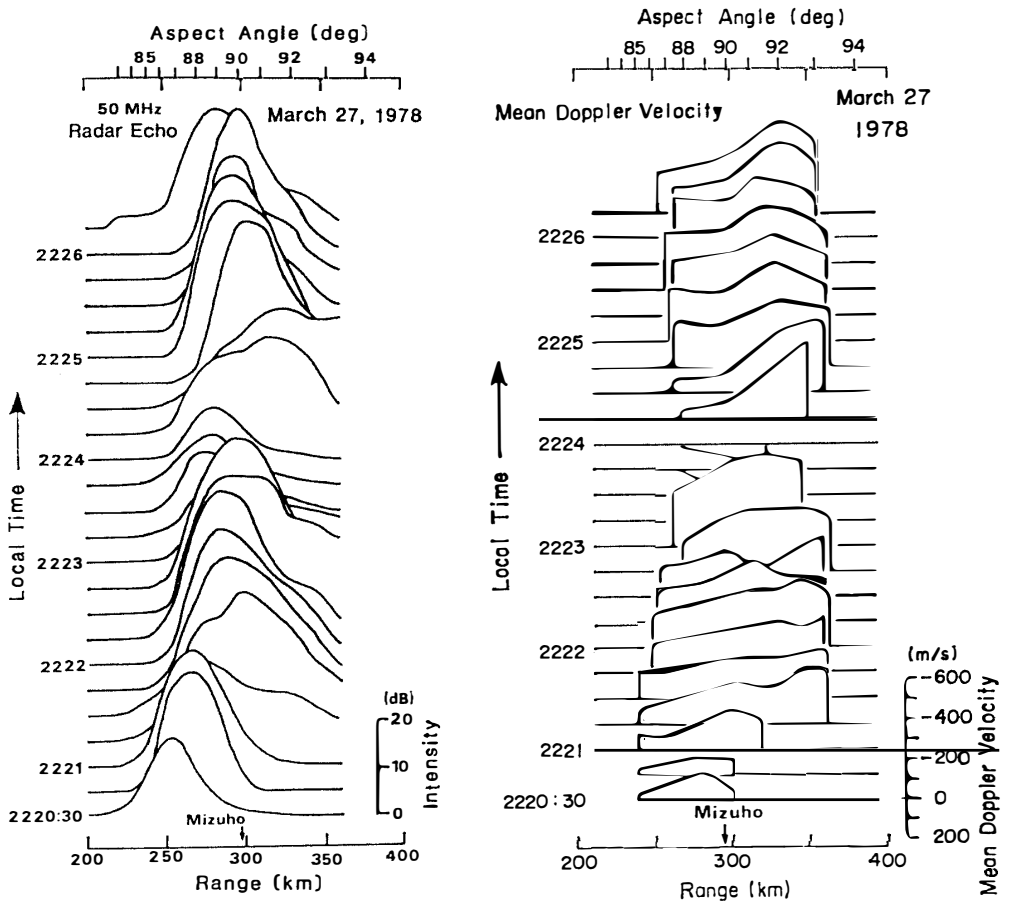

Fig. 6. Range profiles of echo intensity (left) and mean doppler velocity (right) every 15 s. Aspect angle variation with range is shown at the top.

ECKLUND, 1975; GREENWALD *et al.*, 1978; OGAWA *et al.*, 1980). This technique will be also adopted in a new auroral radar system at Syowa Station (IGARASHI *et al.*, 1982).

The left panel in Fig. 6 indicates that except for the echoes between 2220: 30 and 2221: 15 LT most of the echoes come from the 260–330 km range for which the aspect angles are between 88° and 92°. The intensities seems to be maximized for α between 89° and 91°. The limitation of echo intensities within a narrow range of aspect angles is known as 'aspect sensitivity', as has been described in Subsection 2.1.

The echo intensities at times during 2220: 30–2221: 15 LT are maximum around 250–260 km corresponding to the aspect angles of 87°–88° and are very weak around $\alpha=90°$. One possibility to explain this fact is that the aspect angle dependence is seeming, at least, during the time interval of 2220: 30–2221: 15 LT. UNWIN (1966) and OGAWA *et al.* (1982) pointed out that a 50 MHz radar wave may suffer from a refraction of about 1° and 2° during its propagation through the auroral *E*-region with a high electron density. In fact, an extremely high density (about $10^6/cm^3$) was measured in this particular arc by MIYAZAKI *et al.* (1981), indicating that a refraction of about 2° to 3° might occur. If this is the case for our observation, it may be inferred that the aspect angles in the bright arc were near 90° instead of 87°–88°, as the latter values were calculated under an assumption of no radar wave refraction. The refraction effect might be weaker after 2221: 30 LT since important echoes came from the equatorward edge of the arc or outside of it (see Fig. 1).

On the whole, the mean doppler velocities become maximum at ranges farther than those at which the echo intensities are maximum. Since the radar cross-section should be positively correlated with electron drift velocity (SUDAN and KESKINEN, 1979), this discrepancy is curious. One possible explanation is that though the most-irregular region existed at ranges where the mean doppler velocities are maximized, echoes from this region could not be detected due to the aspect sensitivity. The other explanation is that the electric field vector might rotate with range in the horizontal plane. The appropriateness of this possibility, however, cannot be checked since the radar can detect only the east-west component of the electrc field vector. In addition, OGAWA *et al.* (1980) have pointed out the importance of the aspect angle dependence of doppler velocities. Thus, it seems impossible to find a self-consistent explanation for the observed range profiles of both echo intensity and mean doppler velocity by means of only a single radar. A twin-radar system, viewing a common volume from two distant stations, capable of determining electron drift velocity vector, or an experiment in cooperation with an incoherent scatter radar may solve the above problems (ECKLUND *et al.*, 1977; GREENWALD *et al.*, 1978).

3.4. Relations between echo intensity, mean doppler velocity, and spectral width

Despite some limitations (aspect angle dependence and no unique-determination of drift velocity vector) to the explanation of the data, it is valuable to investigate the mutual relations between echo intensity, mean doppler velocity, and spectral width for exploring the characteristics of plasma turbulence associated with aurora. Figure 7 shows the time variations of spectral widths at the 240–360 km range (upper figure) and of both the maximum echo intensity observed in the 255–330 km range and the corresponding doppler velocity (lower figure). It can be observed that after 2221: 15

LT the intensity and velocity variations are positively correlated, whereas the variation of the spectral width has an anti-correlation with that of the echo intensity (and therefore of the velocity). The reason for the opposite correlation before 2221: 15 LT is unknown at this stage but may be attributed to the turbulence in the bright arc being somewhat different from that in other regions.

The echo intensities and spectral widths shown in Fig. 7 are plotted in Fig. 8 as a function of velocity where rough linear-relations are evident (note: echo intensity is in dB). The group of points having narrower spectral width (<150 m/s), higher velocity (<-250 m/s), and stronger intensity (>20 dB) belongs to the category of discrete spectra. On the contrary, the group having wider spectral width (>250 m/s), slower velocity (>-150 m/s), and weaker intensity (<20 dB) falls into the category of diffuse spectra. The echo intensities do not approach the receiver noise level (0 dB) with decreasing velocity, contrary to linear and non-linear theories (SUDAN *et al.*, 1973; SUDAN and KESKINEN, 1979). This contradiction seems to be resolved by assuming a neutral wind blowing from the equator toward the south with a velocity of about 100 m/s (SATO, 1975; OGAWA *et al.*, 1980). Further discussion of this problem, however, is beyond the scope of this paper since there is no experimental data supporting the idea.

Data points in Fig. 8 are replotted logarithmically in Fig. 9 where it can be observed that the echo intensities fall into the region enclosed by two lines, $P=C_1V_d$ and $P=C_2V_d^2$, where P is the intensity (in a dB linear scale), V_d is the mean Doppler velocity, and C_1 and C_2 are proportional constants. This result is roughly consistent

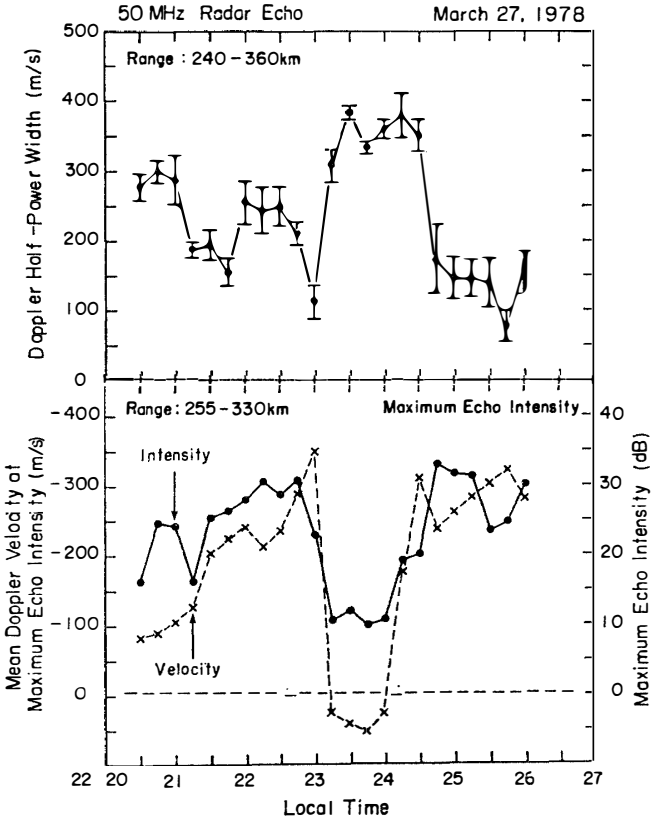

Fig. 7. Time variations of spectral width in the 240–360 km range (upper) and of both the maximum echo intensity observed in the 255–330 km range and corresponding mean doppler velocity (lower). The vertical bars in the upper figure represent standard deviation.

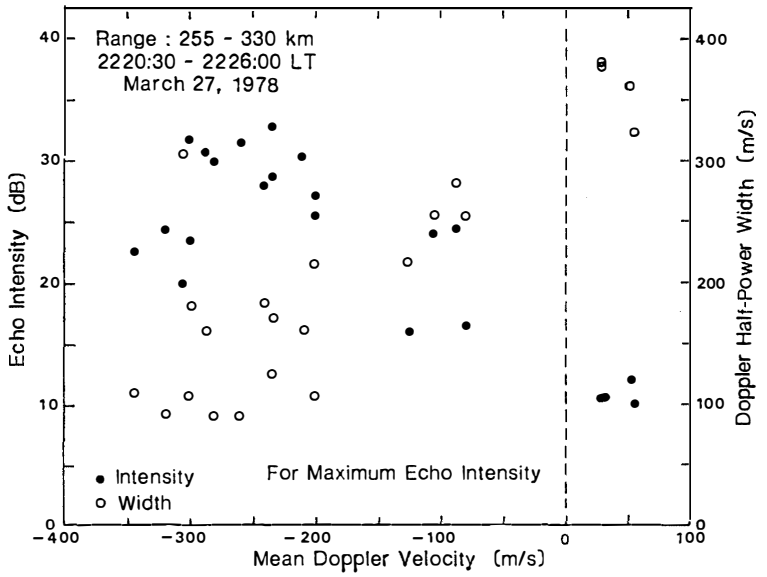

Fig. 8. Plot of the echo intensity and spectral width shown in Fig. 7 as a function of the mean doppler velocity.

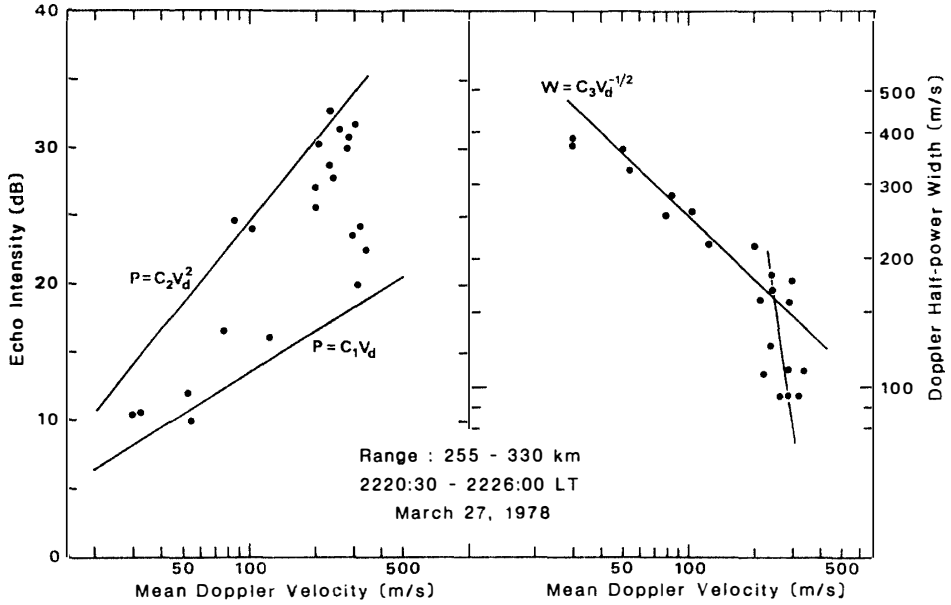

Fig. 9. Replot of the echo intensity and spectral width as a function of the absolute value of the mean doppler velocity shown in Fig. 8. Logarithmic scales are used.

with a relation of $P \propto V_d^2$ in the equatorial electrojet given by BALSLEY (1969) and SUDAN and KESKINEN (1979). The spectral width (W) is almost proportional to $V_d^{-1/2}$ for $V_d \lesssim 250$ m/s and the curve becomes abruptly steeper for V_d beyond about 250 m/s. This means that the spectral forms are completely 'discrete (two-stream-like)' above the turning point of V_d.

V_d must be beyond 350 m/s (ion-acoustic velocity) for the excitation of the two-stream instability in the auroral ionosphere. The turning value of about 250 m/s found above is less than the ion-acoustic velocity. This discrepancy may be explained

partly by the neutral wind effect and partly by the fact that the radar can detect only the north-south component of electron drift velocity vector.

4. Concluding Remarks

The auroral *E*-region irregularities associated with bright arcs have been studied by means of the 50 MHz doppler radar at Syowa Station. The following results are obtained.

(1) Optical aurora is not always spatially collocated with radio aurora. This may suggest that the strong electric field in the lower ionosphere sufficient to excite plasma instabilities has not always an intimate relationship to the magnetospheric electric field which plays an important role in the auroral particle acceleration in the range of a few keV.

(2) The aspect sensitivity limits substantially the echoing region to within the range where aspect angles are 88° to 92°. In order to get a wider coverage in range, the radar beam should be directed geographically southward, in which direction the aspect angle changes more slowly with range than in the present case.

(3) A possibility of a radar wave refraction effect due to high electron density is suggested.

(4) The plasma instabilities causing radar echoes occur and die out within a few seconds or less in accord with the time and spatial variations of electric fields.

(5) The strength of the electric field controls echo intensity, irregularity velocity and spectral form. The intensity and velocity increase with increasing electric field. The spectrum changes from diffuse into discrete form (that is, from wide to narrow spectral width) with increasing electric field. A possibility of the neutral wind effect modifying electron drifts is suggested.

(6) Auroral plasma turbulence is essentially two-dimensional so that a twin-radar system or an experiment in cooperation with an incoherent scatter radar is highly desirable to study detailed turbulent characteristics.

Acknowledgments

We thank all members of the wintering party of the 19th Japanese Antarctic Research Expedition, headed by Prof. T. HIRASAWA, for their kind support to the experiment. We are also grateful to Drs. N. WAKAI and R. MAEDA and Mr. M. OSE of the Radio Research Laboratories for their guidance and support to this study.

References

BALSLEY, B. B. (1969): Some characteristics of non-two-stream irregularities in the equatorial electrojet. J. Geophys. Res., **74**, 2333–2347.

BALSLEY, B. B. and ECKLUND, W. L. (1972): VHF power spectra of the radar aurora. J. Geophys. Res., **77**, 4746–4760.

BALSLEY, B. B., ECKLUND, W. L. and CARTER, D. A. (1977): Dual coherent auroral radar observations from Siple Station, Antarctica. Antarct. J. U. S., **12**, 183–184.

CAHILL, L. T., GREENWALD, R. A. and NIELSEN, E. (1978): Auroral radar and rocket double probe

observations of electric field across the Harang discontinuity. Geophys. Res. Lett., **5**, 687–690.

ECKLUND, W. L., BALSLEY, B. B. and CARTER, D. A. (1977): A preliminary comparison of *F*-region plasma drifts and *E*-region irregularity drifts in the auroral zone. J. Geophys. Res., **82**, 195–197.

FEJER, B. G. and KELLEY, M. C. (1980): Ionospheric irregularities. Rev. Geophys. Space Phys., **18**, 401–454.

GREENWALD, R. A. and ECKLUND, W. L. (1975): A new look at radar auroral motions. J. Geophys. Res., **80**, 3642–3648.

GREENWALD, R. A., WEISS, W., NIELSEN, E. and THOMSON, N. R. (1978): STARE: A new radar auroral backscatter experiment in northern Scandinavia. Radio Sci., **13**, 1021–1039.

HALDOUPIS, C. and SOFKO, G. (1976): Doppler spectrum of 42 MHz CW auroral backscatter. Can. J. Phys., **54**, 1571–1584.

IGARASHI, K. and TSUZURAHARA, S. (1981): Spatial correlations between radio aurora and 4278Å aurora intensity. Mem. Natl Inst. Polar Res., Spec. Issue, **18**, 204–211.

IGARASHI, K., OGAWA, T., TSUZURAHARA, S., SHIRO, I. and OSE, M. (1981): Simultaneous observations of aurora with a doppler-radar and sounding rockets. Mem. Natl Inst. Polar Res., Spec. Issue, **18**, 391–402.

IGARASHI, K., OGAWA, T., OSE, M., FUJII, R. and HIRASAWA, T. (1982): A new VHF doppler radar experiment at Syowa Station, Antarctica. Mem. Natl Inst. Polar Res., Spec. Issue, **22**, 258–267.

KEYS, J. G. and JOHNSTON, P. V. (1979): Radar aurora dynamics as seen by doppler radar. Geophys. Res. Lett., **6**, 97–100.

MIYAZAKI, S., OGAWA, T., MORI, H. and YAMAGISHI, H. (1981): Observational results of electron density profile by S-310JA-7 rocket. Mem. Natl Inst. Polar Res., Spec. Issue, **18**, 300–303.

OGAWA, T., BALSLEY, B. B., ECKLUND, W. L., CARTER, D. A. and JOHNSTON, P. E. (1979): Siple Station auroral radar results: Yearly averaged doppler velocity and echo occurrence patterns. Antarct. J. U. S., **14**, 221–223.

OGAWA, T., BALSLEY, B. B., ECKLUND, W. L., CARTER, D. A. and JOHNSTON, P. E. (1980): Aspect angle dependence of irregularity phase velocities in the auroral electrojet. Geophys. Res. Lett., **7**, 1081–1084.

OGAWA, T., MORI, H., MIYAZAKI, S. and YAMAGISHI, H. (1981a): Electrostatic plasma instabilities in highly active aurora observed by a sounding rocket S-310JA-7. Mem. Natl Inst. Polar Res., Spec. Issue, **18**, 312–329.

OGAWA, T., MAKINO, M., HAYASHIDA, S., YAMAGISHI, H., FUJII, R., FUKUNISHI, H., HIRASAWA, T. and NISHINO, M. (1981b): Measurement of auroral electric fields with an Antarctic sounding rocket S-310JA-7. 1. DC electric field. Mem. Natl Inst. Polar Res., Spec. Issue, **18**, 355–378.

OGAWA, T., BALSLEY, B. B., ECKLUND, W. L., CARTER, D. A. and JOHNSTON, P. E. (1982): Auroral radar observations at Siple Station, Antarctica. J. Atmos. Terr. Phys., **44**, 529–537.

SATO, T. (1975): Neutral winds and electrojet irregularities. J. Geophys. Res., **80**, 2835–2838.

SUDAN, R. N. and KESKINEN, M. J. (1979): Theory of strongly turbulent two-dimensional convection of low-pressure plasma. Phys. Fluids, **22**, 2305–2314.

SUDAN, R. N., AKINRIMISI, J. and FARLEY, D. T. (1973): Generation of small-scale irregularities in the equatorial electrojet. J. Geophys. Res., **78**, 240–248.

UNWIN, R. S. (1966): The importance of refraction in the troposphere and ionosphere in determining the aspect sensitivity and height of the radio aurora. J. Geophys. Res., **71**, 3677–3686.

UNWIN, R. S. and JOHNSTON, P. V. (1981): Height dependence in the power spectrum of diffuse radar aurora. J. Geophys. Res., **86**, 5733–5745.

YAMAGISHI, H., FUKUNISHI, H., HIRASAWA, T. and OGAWA, T. (1981): Measurement of auroral electric fields with an Antarctic sounding rocket S-310JA-7. 2. AC electric field. Mem. Natl Inst. Polar Res., Spec. Issue, **18**, 379–390.

(Received October 30, 1981; Revised manuscript received December 3, 1981)